Cone emission from laser-pumped two-level atoms. II. Analytical model studies

L. You,* J. Mostowski,† and J. Cooper*
Joint Institute for Laboratory Astrophysics, University of Colorado and National Institute of Standards and Technology, Boulder, Colorado 80309-0440
(Received 12 November 1991)

We establish a mechanism, which supports Cherenkov-type radiation, as a source of cone emission. This can be considered as an additional mechanism to the previously discussed four-wave mixing (4WM) and initial encoding and follow-up refraction effects. The radiation source is provided by spontaneous emission of the driven atoms at the frequencies of interest. Due to the medium dispersion, the pump field propagates faster than the phase velocity of the field that is generated at the Rabi sideband at lower frequency. Cherenkov radiation is then possible if the source has a long correlation length, which is indeed the case despite the random nature of spontaneous emission. Coherent superposition of the source for the lower-frequency field is in an off-axis direction given by the Cherenkov radiation condition. Differences between 4WM and Cherenkov-type models are consequently resolved.

PACS number(s): 42.50.Lc, 42.65.−k

I. INTRODUCTION

In spite of the fact that cone emission was first observed over a decade ago [1,2] there is still no generally accepted theory of the effect. In the present paper we detail a mechanism [3] which supports Cherenkov-type radiation [4] due to vacuum fluctuations as a source of cone emission. This can be considered as an additional mechanism to the previously discussed four-wave mixing (4WM) [5], and initial encoding and follow-up refraction effects [6,7]. Due to the medium dispersion the pump field propagates faster than the phase velocity of the field which is generated at the lower-frequency Rabi sideband. Coherent superposition of the radiation from this source then forms the cone. The source of this radiation has been identified in the preceding paper [8] (hereafter referred to as paper I), where it is shown to be provided by spontaneous emission of the driven atoms at the frequencies of interest. Cherenkov radiation is then possible if the source has a long correlation length (contrary to Valley *et al.* [9], where such a source is assumed to be δ correlated), which is indeed the case despite the random nature of spontaneous emission. This radiation source enters into the equations for the fields in the same form as the source generated by four-wave mixing and therefore might be considered as a "spontaneous four-wave mixing," since the photons emitted in the Rabi sidebands are correlated. However, in general, in more complicated systems (e.g., a three-level Λ-type system) or when collisions are present, such a source exists even in the absence of 4WM.

In paper I [8], we formulated the theoretical treatment of the problem. We treated the strong pump field classically and found that its equations of propagation coupled to the steady-state equations of the atomic operators are

$$\left[\nabla_T^2-2ik_p\left[\frac{\partial}{\partial z}+\frac{1}{v_p}\frac{\partial}{\partial t}\right]\right]\hat{\Omega}_p^{(-)}=-\frac{4\pi N\omega_p^2|\mathbf{d}_{21}|^2}{c^2\hbar}\hat{\sigma}_{21}^s\ , \tag{1.1}$$

$$\hat{\sigma}_{21}^s=-\frac{\omega_0\left[\Delta+i\frac{\gamma}{2}\right]}{\Delta^2+\frac{\gamma^2}{4}+\frac{|\Omega_p|^2}{2}2}\ .$$

These equations allow us to solve for the pump field first, and then find the steady-state values of the atomic operators. To first order in the generated fields, we have the following steady-state propagation operator equations for the slowly varying copropagating quantum fields of interest:

$$\left[\nabla_T^2-2ik_s\frac{\partial}{\partial z}\right]\hat{\Omega}_s^{(-)}=-\alpha_s\hat{\Omega}_s^{(-)}+\kappa_4\hat{\Omega}_4^{(+)}+\hat{\beta}_s\ ,$$
$$\left[\nabla_T^2+2ik_4\frac{\partial}{\partial z}\right]\hat{\Omega}_4^{(+)}=-\alpha_4^*\hat{\Omega}_4^{(+)}+\kappa_s^*\hat{\Omega}_s^{(-)}+\hat{\beta}_4^\dagger\ . \tag{1.2}$$

All notation and symbols are the same as in paper I, except here we have neglected the + indexing of copropagating sources because we only discuss one-way propagation. The dependence on τ has also been suppressed, since we only discuss the steady-state limit ($\tau\rightarrow\infty$). The noise terms in the above are proven to have a long coherence length compared with a typical cell length employed in most experiments, and we have

$$\langle\hat{\beta}_s(\mathbf{r})\hat{\beta}_s^\dagger(\mathbf{r}')\rangle=\zeta^2(\omega_s)|\mathcal{D}_s^{(+)}|^2D_s(\mathbf{r},\mathbf{r}')\ ,$$
$$\langle\hat{\beta}_4^\dagger(\mathbf{r})\hat{\beta}_4(\mathbf{r}')\rangle=\zeta^2(\omega_4)|\mathcal{D}_4^{(-)}|^2D_s(\mathbf{r},\mathbf{r}')\ ,$$
$$\langle\hat{\beta}_s(\mathbf{r})\hat{\beta}_4(\mathbf{r}')\rangle=\zeta(\omega_s)\zeta(\omega_4)\mathcal{D}_s^{(+)}\mathcal{D}_4^{(-)}D_s(\mathbf{r},\mathbf{r}')\ , \tag{1.3}$$
$$\langle\hat{\beta}_4^\dagger(\mathbf{r})\hat{\beta}_s^\dagger(\mathbf{r}')\rangle=\zeta(\omega_s)\zeta(\omega_4)(\mathcal{D}_s^{(+)}\mathcal{D}_4^{(-)})^*D_s(\mathbf{r},\mathbf{r}')\ ,$$

and

$$\begin{aligned}
&\langle\hat{\beta}_4(\mathbf{r})\hat{\beta}_4^{\dagger}(\mathbf{r}')\rangle=\zeta^2(\omega_4)|\mathcal{D}_4^{(+)}|^2D_4(\mathbf{r},\mathbf{r}')\ ,\\
&\langle\hat{\beta}_s^{\dagger}(\mathbf{r})\hat{\beta}_s(\mathbf{r}')\rangle=\zeta^2(\omega_s)|\mathcal{D}_s^{(-)}|^2D_4(\mathbf{r},\mathbf{r}')\ ,\\
&\langle\hat{\beta}_4(\mathbf{r})\hat{\beta}_s(\mathbf{r}')\rangle=\zeta(\omega_s)\zeta(\omega_4)\mathcal{D}_s^{(-)}\mathcal{D}_4^{(+)}D_4(\mathbf{r},\mathbf{r}')\ ,\\
&\langle\hat{\beta}_s^{\dagger}(\mathbf{r})\hat{\beta}_4^{\dagger}(\mathbf{r}')\rangle=\zeta(\omega_s)\zeta(\omega_4)(\mathcal{D}_s^{(-)}\mathcal{D}_4^{(+)})^*D_4(\mathbf{r},\mathbf{r}')\ .
\end{aligned}\tag{1.4}$$

Under the paraxial approximation (PA),

$$D_j(\mathbf{r},\mathbf{r}')=\frac{4}{\hbar}\frac{|\mathbf{d}_{21}|^2}{(2\pi c)^3}\frac{\pi^2}{\Gamma_j}\frac{1}{ik_j(z-z')+k_j^2a^2}\times\exp\left[-\frac{(k_j|\delta\boldsymbol{\rho}|)^2}{2[ik_j(z-z')+k_j^2a^2]}\right]\ .\tag{1.5}$$

In this paper we point out that a Cherenkov-type emission mechanism not considered by Valley *et al.* [9] should also be taken into account when discussing cone emission. This effect relates to the initiation and generation of the frequency-shifted beams and is intrinsically quantum in nature. It comes from the spatial correlation at different positions of the polarization of the medium generated by spontaneous emission at the relevant frequencies as we described in paper I. In that paper we showed, by explicit calculation, that due to the interaction with the electromagnetic field, the polarization of the medium has a large correlation length, contrary to the δ-correlated assumption of Valley *et al.* [9]. Our results show that the source, i.e., the $\hat{\beta}_j$ in the above equations, although quantum in nature, is effectively a coherent source. This permits us to give a clear physical picture of the cone emission and also unifies most of the previous simple model studies. The differences between 4WM and Cherenkov-type radiation models can then be clearly defined.

This paper is organized as follows. In Sec. II model studies without 4WM are described to elucidate the significance of the long-coherence-length quantum noise and a physical picture of Cherenkov-type cone emission is presented. In Sec. III model studies are conducted to explore the role played by 4WM. In Sec. IV we compare the present results with previous models on cone emission. Conclusions are presented in Sec. V.

II. MODEL STUDIES WITHOUT 4WM

To gain some insight into the solution of Eqs. (1.2), we first study them perturbatively. Neglecting the mixing with the wave $\hat{\Omega}_4^{(+)}$, we can write the equation for $\hat{\Omega}_s^{(-)}$ as

$$\left[\nabla_T^2-2ik_s\frac{\partial}{\partial z}\right]\hat{\Omega}_s^{(-)}(\boldsymbol{\rho},z)=-\alpha_s\hat{\Omega}_s^{(-)}(\boldsymbol{\rho},z)+\hat{\beta}_s(\boldsymbol{\rho},z)\ ,\tag{2.1}$$

which describes the generation of $\hat{\Omega}_s^{(-)}$ field via $\chi^{(3)}$ induced by the pump (i.e., the α_s coefficient in the above equation). We take α_s to be a real constant because we are interested in the phase which determines the spatial propagation direction (note that the imaginary part will contribute to the gain or loss of the field). This equation can then be solved (see Appendix A), and the solution is

$$\hat{\Omega}_s^{(-)}(\boldsymbol{\rho},z)=\frac{ik_s}{2\pi}\int_0^z\int_{A'}\frac{1}{z-z'}e^{-(i\alpha_s/2k_s)(z-z')}\times e^{-i[k_s|\boldsymbol{\rho}-\boldsymbol{\rho}'|^2/2(z-z')]}\times\hat{\beta}_s(\boldsymbol{\rho}',z')dz'd\boldsymbol{\rho}'\tag{2.2}$$

with the boundary condition $\hat{\Omega}_s^{(-)}(\boldsymbol{\rho}',0)=0$. As defined in paper I, $\hat{\Omega}_s^{(+-)}$ describes the generated quantum fields, consequently this boundary condition reflects the fact that $\hat{\Omega}_s^{(-)}$ is zero at the input face. However, the total field at this frequency is, as required, $\hat{\Omega}_s^{(\pm)}+\hat{\Omega}_{s\,\mathrm{vac}}^{(\pm)}$ [from Eq. (6.44) in paper I], therefore

$$[\hat{\Omega}_s^{(-)}(\boldsymbol{\rho},z)+\hat{\Omega}_{s\,\mathrm{vac}}^{(-)}(\boldsymbol{\rho},z),\hat{\Omega}_s^{(+)}(\boldsymbol{\rho}',z')+\hat{\Omega}_{s\,\mathrm{vac}}^{(+)}(\boldsymbol{\rho}',z')]\neq0\ .\tag{2.3}$$

In most of the cases, we are not interested in the intensity at the exit window of the medium, instead we observe the intensity in the far-field limit. We also assume that the field propagates to the far field from the exit window according to the Huygens principle [10], then

$$\hat{\Omega}_s^{(-)}(\boldsymbol{\rho},Z)\sim\int_A\frac{1}{|\mathbf{R}-\boldsymbol{\rho}_1-L\hat{e}_z|}e^{-ik_s|\mathbf{R}-\boldsymbol{\rho}_1-L\hat{e}_z|}\times\hat{\Omega}_s^{(-)}(\boldsymbol{\rho}_1,L)e^{i\omega_s\tau}d\boldsymbol{\rho}_1\ ,\tag{2.4}$$

where A is the area of the cell exit window (A' being the cross section inside the cell). The geometry gives (see Fig. 1)

$$\mathbf{R}=(Z+L)\hat{e}_z+\rho\hat{e}_\rho\ .\tag{2.5}$$

We are only interested in the region where $Z\gg L$ and $Z\gg\rho$; then

$$\frac{1}{|\mathbf{R}-\boldsymbol{\rho}_1-L\hat{e}_z|}\approx\frac{1}{Z}\ ,\tag{2.6}$$

and

$$k_s|\mathbf{R}-\boldsymbol{\rho}_1-L\hat{e}_z|\approx k_sZ+\frac{k_s}{2Z}|\boldsymbol{\rho}-\boldsymbol{\rho}_1|^2+\cdots\ .\tag{2.7}$$

We obtain

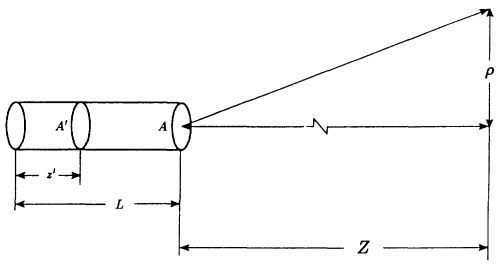

FIG. 1. Far-field geometry.

$$\hat{\Omega}_s^{(-)}(\boldsymbol{\rho},Z)\sim\frac{1}{Z}\int_A e^{-ik_sZ-i(k_s/2Z)|\boldsymbol{\rho}-\boldsymbol{\rho}_1|^2}e^{i\omega_s\tau}\hat{\Omega}_s^{(-)}(\boldsymbol{\rho}_1,L)d\boldsymbol{\rho}_1$$
$$=\frac{1}{Z}\frac{ik_s}{2\pi}\int_A e^{-ik_sZ-i(k_s/2Z)|\boldsymbol{\rho}-\boldsymbol{\rho}_2|^2}e^{i\omega_s\tau}d\boldsymbol{\rho}_1\int_0^z\int_{A'}\frac{1}{L-z'}e^{-(i\alpha_s/2k_s)(L-z')}e^{-i[k_s|\boldsymbol{\rho}_1-\boldsymbol{\rho}'_1|^2/2(L-z')]}\hat{\beta}_s(\boldsymbol{\rho}'_1,z')dz'd\boldsymbol{\rho}'_1\ . \tag{2.8}$$

Now we can transform to the dimensionless coordinates

$$z\to zL,\quad Z\to ZL,\quad \rho\to\rho\rho_0\ , \tag{2.9}$$

where L is the length of the cell, and ρ_0 is the Gaussian waist of the pump beam.

We also define the following:

$$\mathcal{F}_s=\frac{2L}{k_s\rho_p^2}\approx\frac{2L}{k_p\rho_p^2}\quad\text{(Fresnel number)}\ ,\quad \bar{\alpha}_s=\frac{\alpha_sL}{2k_s}\ . \tag{2.10}$$

With the change of variable $1-z'\to z'$, we obtain

$$\hat{\Omega}_s^{(-)}(\boldsymbol{\rho},Z)\sim\frac{ik_s\rho_p^2}{2\pi ZL}e^{-ik_sZL+i\omega_s\tau}\bar{\hat{\Omega}}_s^{(-)}(\boldsymbol{\rho},Z)\ , \tag{2.11}$$

with

$$\bar{\hat{\Omega}}_s^{(-)}(\boldsymbol{\rho},Z)=\int_A e^{-i(|\boldsymbol{\rho}-\boldsymbol{\rho}_1|^2/\mathcal{F}_sZ)}d\boldsymbol{\rho}_1\int_0^1\int_{A'}\frac{1}{z'}e^{-i\bar{\alpha}_sz'}e^{-i(|\boldsymbol{\rho}_1-\boldsymbol{\rho}'_1|^2/\mathcal{F}_sz')}\hat{\beta}_s(\boldsymbol{\rho}'_1,z')dz'd\boldsymbol{\rho}'_1\ . \tag{2.12}$$

The intensity distribution in the transverse direction in the far field is then given by

$$I_s(\boldsymbol{\rho},Z)\sim\langle\hat{\Omega}_s^{(-)}(\boldsymbol{\rho},Z)\hat{\Omega}_s^{(+)}(\boldsymbol{\rho},Z)\rangle$$
$$\sim\int_A\int_A e^{-i(|\boldsymbol{\rho}-\boldsymbol{\rho}_1|^2/\mathcal{F}_sZ)+i(|\boldsymbol{\rho}-\boldsymbol{\rho}_2|^2/\mathcal{F}_sZ)}d\boldsymbol{\rho}_1d\boldsymbol{\rho}_2$$
$$\times\int_0^1\int_0^1\frac{1}{z'_1z'_2}e^{-i\bar{\alpha}_sz'_1+i\bar{\alpha}_sz'_2}dz'_1dz'_2$$
$$\times\int_{A'}\int_{A'}e^{-i(|\boldsymbol{\rho}_1-\boldsymbol{\rho}'_1|^2/\mathcal{F}_sz'_1)+i(|\boldsymbol{\rho}-\boldsymbol{\rho}'_2|^2/\mathcal{F}_sz'_2)}d\boldsymbol{\rho}'_1d\boldsymbol{\rho}'_2\langle\hat{\beta}_s(\boldsymbol{\rho}'_1,z'_1)\hat{\beta}_s^{\dagger}(\boldsymbol{\rho}'_2,z'_2)\rangle\ . \tag{2.13}$$

Here $\langle\ \rangle$ represents the quantum expectation value.

The source is present only in the region illuminated by the pump, and therefore has finite transverse dimension, which is governed by the prefactors $\mathcal{D}_j^{(\pm)}$ in the $\hat{\beta}_j$ due to $\hat{w}^s(\mathbf{r})$ and $\hat{\sigma}_{21}^s(\mathbf{r})$, etc. They are determined by the shape of the transverse pump field. We assume that in the self-trapped filaments, the transverse shape is Gaussian. Then we can put

$$\hat{\beta}_s(\boldsymbol{\rho},z)=e^{-\rho^2}\bar{\hat{\beta}}_s(\boldsymbol{\rho},z)\ . \tag{2.14}$$

We now perform model studies to determine how the cones are generated.

A. Coherent source

The correlation function under the PA is given in Eq. (1.5). For a long sample whose transverse dimension is determined by ρ_0, we would expect the source $\hat{\beta}_s$ to be present only along this filament. The coarse-graining radius a can be of the same order of magnitude as the waist ρ_0 of the pump beam in the self-focusing medium. For a relatively long cell, we would expect contributions from all along the filament, consequently the argument in the exponential in Eq. (1.5) will be small, and an adequate approximation close to the axis will be

$$D_s=\frac{4}{\hbar}\frac{|\mathbf{d}_{21}|^2}{(2\pi c)^3}\frac{\pi^2}{\Gamma_s}\frac{1}{ik_sL(z-z')+k_s^2a^2}\ , \tag{2.15}$$

which can be further approximated by

$$\langle\bar{\hat{\beta}}_s(\boldsymbol{\rho},z)\bar{\hat{\beta}}_s{}^{\dagger}(\mathbf{p}',z')\rangle=\text{const}\ , \tag{2.16}$$

for $|z-z'|<k_s\rho_0^2/L$, which is the (scaled) Rayleigh length. This approximation will be more fully tested numerically. Thus we first assume it to be a coherent source

$$\bar{\hat{\beta}}_s(\boldsymbol{\rho},z)=\text{const} \tag{2.17}$$

independent of ρ and z provided $|z-z'|<k_s\rho_0^2/L$.

We can work with the field directly, then Eq. (2.12) reduces to

$$\bar{\hat{\Omega}}_s^{(-)}(\boldsymbol{\rho},Z)\sim\int_A e^{-i(|\boldsymbol{\rho}-\boldsymbol{\rho}_1|^2/\mathcal{F}_sZ)}d\boldsymbol{\rho}_1$$
$$\times\int_0^1\int_{A'}\frac{1}{z'}e^{-i\bar{\alpha}_sz'}e^{-i(|\boldsymbol{\rho}_1-\boldsymbol{\rho}'_1|^2/\mathcal{F}_s^{z'})}$$
$$\times e^{-\rho'^2}dz'd\boldsymbol{\rho}'_1\ , \tag{2.18}$$

since $Z \gg z' \in [0,1]$ (see Appendix B). We obtain

$$\bar{\hat{\Omega}}_s^{(-)}(\boldsymbol{\rho},Z) \sim e^{-\rho^2/(\mathcal{F}_s Z)^2} e^{-i(\eta/2)} \frac{2\sin\frac{\eta}{2}}{\eta} , \tag{2.19}$$

where

$$\eta = \bar{\alpha}_s - \frac{\mathcal{F}_s \rho^2}{(\mathcal{F}_s Z)^2} . \tag{2.20}$$

When $\eta = \mathrm{mod}(\pi,0)$, we have series of maxima. The first maximum is at $\eta=0$. Therefore the angular distribution of radiation has the form of a cone with the cone angle (see Fig. 2),

$$\theta_c \approx \frac{\rho\rho_0}{ZL} = \sqrt{\bar{\alpha}_s \mathcal{F}_s}\frac{\rho_0}{L} = \sqrt{\alpha_s}/k_s \approx \sqrt{2(n_s-1)} . \tag{2.21}$$

Here $n_s(\omega_s)$ is the phenomenological index of refraction of the s wave; the index of refraction at the frequency of the pump field has been taken to be 1. We will compare this simple formula with various other models in Sec. III. (Of course the intensity also contains a Gaussian prefactor which will give the overall amplitude of the profile. In fact, the intensity resulting from Eq. (2.15) contains factors associated with $|z-z'| < k_j\rho_0^2/L$ from the z and z' integrals which gives a prefactor of approximately $Lk_j\rho_0^2$ on axis. The intensity is modulated by the diffraction pattern associated with the exit aperture of area $A=\pi\rho_0^2$, which gives the first minimum at $\theta_d \approx 1/(k_s\rho_0)$. Of course, we require $\theta_c < \theta_d$ for observability of the cone.)

B. White-noise source

We now assume that $\hat{\beta}_s$ is a δ-correlated incoherent source. This is generally not applicable for the realistic case, and we discuss it here only for comparison. Then with

$$\langle \bar{\hat{\beta}}_s(\boldsymbol{\rho},z)\bar{\hat{\beta}}_s^{\dagger}(\boldsymbol{\rho}',z')\rangle \sim \delta(\boldsymbol{\rho}-\boldsymbol{\rho}')\delta(z-z') , \tag{2.22}$$

we obtain (Appendix C)

$$I_s(\boldsymbol{\rho},Z) \sim \frac{\pi^3 \mathcal{F}_s^2 Z}{2(1+Z)} . \tag{2.23}$$

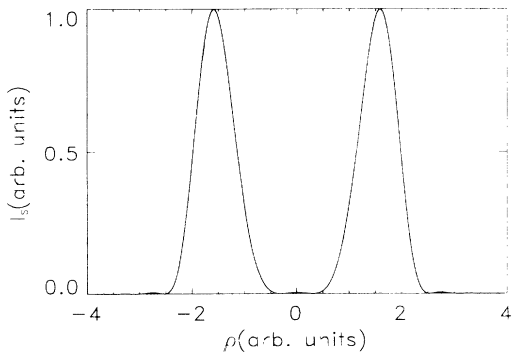

FIG. 2. Typical cross section of the cylindrical symmetric far-field intensity distribution of the redshifted field due to a noise source with long correlation length.

The intensity does not depend on the transverse variables, which indicates that the angular distribution is flat (apart from the overall modulation due to the diffraction pattern associated with the exit source of area $A=\pi\rho_0^2$). This is of course due to the oversimplification of this model calculation. However, we emphasize that Eq. (2.22) is equivalent to the initiation of the noise proposed by Valley *et al.* [9]. It illustrates that the cone obtained in case II A is due to the coherence of the dipole polarization throughout the medium.

A different approximation has also been made to α. As is often valid in optical fibers, we put $\alpha(\boldsymbol{\rho}) = \alpha_0(1-\rho^2)$. The field equation can still be solved for the δ-correlated case as in Eq. (2.22), but again no cone structure is found.

C. General partially coherent source

To obtain an understanding of the effect of the coherence length, we treat the case of a partially coherent source. We emphasize, however, that case II A is actually the physically relevant approximate result for the problem under consideration in this paper. We then take

$$\langle \bar{\hat{\beta}}_s(\boldsymbol{\rho},z)\bar{\hat{\beta}}_s^{\dagger}(\mathbf{p}',z')\rangle \sim e^{-(1/\lambda_c)|\rho\rho_0+\hat{e}_z zL-\rho'\rho_0-\hat{e}_x z'L|} . \tag{2.24}$$

We have demonstrated numerically that in the far field a conical distribution is a generic feature. To simplify analytical calculations, we assume Eq. (2.24) is factorizable into transverse and longitudinal directions; then we have

$$\langle \bar{\hat{\beta}}_s(\boldsymbol{\rho},z)\bar{\hat{\beta}}_s^{\dagger}(\mathbf{p}',z')\rangle \sim e^{-(1/\lambda_\perp)|\rho-\rho'|} e^{-(1/\lambda_\parallel)|z-z'|} , \tag{2.25}$$

with $\lambda_\perp$ and $\lambda_\parallel$ in units of ρ_0 and L, respectively.

We obtain (Appendix D)

$$I_s(\boldsymbol{\rho},Z) \sim \mathcal{R}Z , \tag{2.26}$$

with

$$\mathcal{R} \sim \int_0^\infty e^{-(1-i/\mathcal{F}_s Z)\rho'^2-(i+1/\mathcal{F}_s Z)^2\rho'^2} \times J_0\left[2\frac{\rho\rho'}{\mathcal{F}_s Z}\right] e^{-(1/\lambda_\perp)\rho'}\rho' d\rho' ,$$

$$Z = \int_0^1\int_0^1 e^{-i(\bar{\alpha}_s-\rho^2/\mathcal{F}_s Z^2)(z_1'-z_2')} e^{-(1/\lambda_\parallel)|z_1'-z_2'|} dz_1' dz_2' , \tag{2.27}$$

where $\mathcal{R}$ is a slowly varying function of Z and ρ. Changing the integration variables to z_1' and $z'=z_2'-z_1'$, we obtain

$$\mathcal{Z}=\int_0^1 dz_1'\int_{-z_1'}^0 e^{i\eta z'}e^{(1/\lambda_\parallel)z'}dz'+\int_0^1 dz_1'\int_0^{1-z_1'} e^{i\eta z'}e^{-(1/\lambda_\parallel)z'}dz'$$

$$=\int_0^1 dz_1'\left[\frac{1-e^{-i\eta z_1'-(1/\lambda_\parallel)z_1'}}{i\eta+\frac{1}{\lambda_\parallel}}-\frac{1-e^{i\eta(1-z_1')-(1/\lambda_\parallel)(1-z_1')}}{i\eta-\frac{1}{\lambda_\parallel}}\right]$$

$$=\frac{2\lambda_\parallel}{\eta^2\lambda_\parallel^2+1}+\frac{2\lambda_\parallel^2(\eta^2\lambda_\parallel^2-1)}{(\eta^2\lambda_\parallel^2+1)^2}+\frac{2\lambda_\parallel^2 e^{-1/\lambda_\parallel}}{\eta^2\lambda_\parallel^2+1}\cos(\eta+\psi)\ , \tag{2.28}$$

with $\psi=2\tan^{-1}(\eta\lambda_\parallel)$.

This expression indeed reduces to the previous two cases when we put $\lambda_\parallel\to\infty$ for a coherent source [Eq. (2.16)], and $\lambda_\parallel\to 0$ for a white-noise source [Eq. (2.22)], respectively.

The cone will appear around $\eta+\psi(\eta)=0$. As $\eta\to 0$, $\psi(\eta)\to 0$, and this will give

$$\theta_c=\sqrt{2(n_s-1)}\ , \tag{2.29}$$

which is the same as previously obtained. In general we expect cones, but their contrast against the background decays rapidly (roughly as $e^{-1/\lambda_\parallel}$). For the completely coherent source ($\lambda_\parallel\to\infty$), the contrast of the cone is largest. In Fig. 3 we have plotted the far-field intensity distribution Eq. (2.26) versus correlation length $\lambda_\parallel$, with the $\mathcal{Z}$ as given by Eq. (2.28), and the overall Gaussian profile given by $\mathcal{R}$ as in Eq. (2.19), which corresponds to $\lambda_\perp\to\infty$.

III. MODEL STUDIES WITH 4WM

To examine the differences due to 4WM in more detail, we consider a simple model study including the 4WM perturbatively. The coupled equations (1.2) can be solved by combined Fourier transform ($\mathcal{F}$) of the transverse coordinates ($\boldsymbol{\rho}$) and Laplace transformation ($\mathcal{L}$) of the longitudinal coordinate (z),

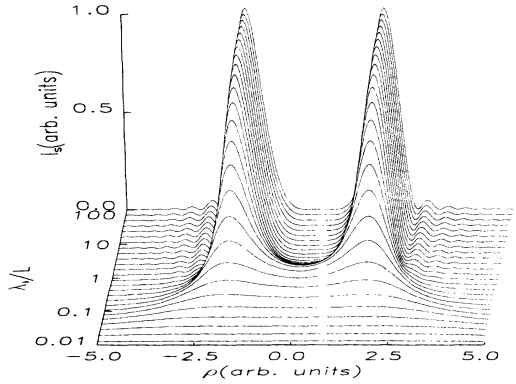

FIG. 3. The dependence of the far-field intensity distribution on the correlation length of the noise source.

$$\mathcal{L}[\hat{O}(z)]=\hat{O}(q)=\int_0^\infty e^{-qz}\hat{O}(z)dz\ ,$$

$$\mathcal{F}[\hat{O}(\boldsymbol{\rho})]=\hat{O}(\mathbf{k}_\perp)=\frac{1}{2\pi}\int_{A'}e^{i\mathbf{k}_\perp\cdot\boldsymbol{\rho}}\hat{O}(\boldsymbol{\rho})d\boldsymbol{\rho}\ ,$$

$$\mathcal{L}[\mathcal{F}\hat{O}(\boldsymbol{\rho},z)]=\hat{O}(\mathbf{k}_\perp,q)$$

$$=\frac{1}{2\pi}\int_0^\infty e^{-qz}dz\int_{A'}e^{i\mathbf{k}_\perp\cdot\boldsymbol{\rho}}\hat{O}(\boldsymbol{\rho},z)d\boldsymbol{\rho}\,dz\ , \tag{3.1}$$

where $\hat{O}$ represents any one of $\hat{\Omega}_s^{(-)}$, $\hat{\Omega}_4^{(+)}$, $\hat{\beta}_s$, or $\hat{\beta}_4^\dagger$. Again take α_s, α_4^*, κ_s^*, and κ_4 as real constants. With the appropriate boundary conditions, we get the following algebraic equations:

$$(-2ik_sq-k_\perp^2)\hat{\Omega}_s^{(-)}(\mathbf{k}_\perp,q)$$
$$=-\alpha_s\hat{\Omega}_s^{(-)}(\mathbf{k}_\perp,q)+\kappa_4\hat{\Omega}_4^{(+)}(\mathbf{k}_\perp,q)+\hat{\beta}_s(\mathbf{k}_\perp,q)\ , \tag{3.2}$$

$$(2ik_4q-k_\perp^2)\hat{\Omega}_4^{(+)}(\mathbf{k}_\perp,q)$$
$$=-\alpha_4^*\hat{\Omega}_4^{(+)}(\mathbf{k}_\perp,q)+\kappa_s^*\hat{\Omega}_s^{(-)}(\mathbf{k}_\perp,q)+\hat{\beta}_4^\dagger(\mathbf{k}_\perp,q)\ .$$

The solution is

$$\begin{bmatrix}\hat{\Omega}_s^{(-)}(\mathbf{k}_\perp,q)\\ \hat{\Omega}_4^{(+)}(\mathbf{k}_\perp,q)\end{bmatrix}=M^{-1}\begin{bmatrix}\hat{\beta}_s(\mathbf{k}_\perp,q)\\ \beta_4^\dagger(\mathbf{k}_\perp,q)\end{bmatrix}\ . \tag{3.3}$$

Here M^{-1} is the inverse of M, and

$$M=\begin{bmatrix}-2ik_sq-k_\perp^2+\alpha_s & -\kappa_4\\ -\kappa_s^* & 2ik_4q-k_\perp^2+\alpha_4^*\end{bmatrix}\ , \tag{3.4}$$

$$M^{-1}=\frac{1}{\det(M)}\begin{bmatrix}2ik_4q-k_\perp^2+\alpha_4^* & \kappa_4\\ \kappa_s^* & -2ik_sq-k_\perp^2+\alpha_s\end{bmatrix}\ , \tag{3.5}$$

where

$$\det(M)=4k_sk_4\left[q^2+q(q_s+q_4)+q_sq_4-\frac{\kappa_s^*\kappa_4}{4k_sk_4}\right]\ , \tag{3.6}$$

with

$$q_s = i\frac{-k_\perp^2+\alpha_s}{2k_s} ,$$
$$q_4 = -i\frac{-k_\perp^2+\alpha_4^*}{2k_4} . \tag{3.7}$$

We see in general that the $\hat{\Omega}_s^{(-)}$ field comes from both source terms due to 4WM. It is given explicitly by

$$\hat{\Omega}_s^{(-)}(\mathbf{k}_\perp,q)=\frac{1}{\det(M)}[(-2ik_4q-k_\perp^2-\alpha_4^*)\hat{\beta}_s(\mathbf{k}_\perp,q) + \kappa_4\hat{\beta}_4^\dagger(\mathbf{k}_\perp,q)] . \tag{3.8}$$

To avoid complications due to the presence of both the Cherenkov-type source $\hat{\beta}_s$ and the 4WM source term $\hat{\beta}_4^\dagger$ for $\hat{\Omega}_s^{(-)}$ field, we will put $\hat{\beta}_s=0$, and focus on the 4WM source $\hat{\beta}_4^\dagger$. In fact the first term in Eq. (3.8) will reproduce all the results discussed in Sec. II. Then

$$\hat{\Omega}_s^{(-)}(\mathbf{k}_\perp,q)=\frac{1}{\det(M)}\kappa_4\hat{\beta}_4^\dagger(q,\mathbf{k}_\perp) . \tag{3.9}$$

The above solution is, in general, too complicated to invert into real space. In order to gain an understanding of the initiation process, we look at the weak-coupling limit, defined by

$$|\kappa_4| \ll |\alpha_s| ,$$
$$|\kappa_s^*| \ll |\alpha_4^*| . \tag{3.10}$$

Then we obtain

$$\hat{\Omega}_s^{(-)}(\mathbf{k}_\perp,q)\approx\frac{\kappa_4}{4k_sk_4(q+q_s)(q+q_4)}\hat{\beta}_4^\dagger(\mathbf{k}_\perp,q) . \tag{3.11}$$

Now the inverse of the Laplace transform ($\mathcal{L}^{-1}$) can be carried out explicitly as [11]

$$\mathcal{L}^{-1}\left[\frac{1}{(q+q_s)(q+q_4)}\right]=\frac{e^{-q_sz}-e^{-q_4z}}{q_4-q_s} , \tag{3.12}$$

from which we get for the field

$$\hat{\Omega}_s^{(-)}(\boldsymbol{\rho},z)=\frac{\kappa_4}{4k_sk_4}\int dz'\int_{A'}e^{-i\mathbf{k}_\perp\cdot\boldsymbol{\rho}}d\mathbf{k}_\perp\frac{e^{-q_s(z-z')}-e^{-q_4(z-z')}}{q_4-q_s}\int_{A'}e^{i\mathbf{k}_\perp\cdot\boldsymbol{\rho}'}d\mathbf{p}'\hat{\beta}_4^\dagger(\boldsymbol{\rho}',z') . \tag{3.13}$$

In the paraxial limit, we have $|\alpha_s| \gg q_s$ and $|\alpha_4^*| \gg q_4$. Then

$$q_4-q_s=-i\left[\frac{-k_\perp^2+\alpha_4^*}{2k_4}+\frac{-k_\perp^2+\alpha_s}{2k_s}\right]\approx -i\left[\frac{\alpha_4^*}{2k_4}+\frac{\alpha_s}{2k_s}\right]=\text{const} . \tag{3.14}$$

We therefore get the following after the integration over the angle of $\mathbf{k}_\perp$ relative to $\boldsymbol{\rho}-\boldsymbol{\rho}'$:

$$\hat{\Omega}_s^{(-)}(\boldsymbol{\rho},z)\sim\frac{\kappa_4}{4k_sk_4}\int dz'\int_{A'}d\boldsymbol{\rho}'\int_0^\infty(e^{-q_s(z-z')}-e^{-q_4(z-z')})J_0(k_\perp|\boldsymbol{\rho}-\boldsymbol{\rho}'|)k_\perp dk_\perp\hat{\beta}_4^\dagger(\mathbf{p}',z') . \tag{3.15}$$

The integration over $k_\perp$ is of exactly the same form as Eq. (A8), and appropriate substitution will give us the following solution:

$$\hat{\Omega}_s^{(-)}(\boldsymbol{\rho},z)=\hat{\Omega}_{s1}^{(-)}(\boldsymbol{\rho},z)+\hat{\Omega}_{s2}^{(-)}(\boldsymbol{\rho},z) , \tag{3.16}$$

where (for $z<1$)

$$\hat{\Omega}_{s1}^{(-)}(\boldsymbol{\rho},z)\sim\int dz'\int_{A'}d\boldsymbol{\rho}'\frac{1}{z-z'}k_s\exp\left[-i\frac{\alpha_s(z-z')}{2k_s}-i\frac{k_s|\boldsymbol{\rho}-\boldsymbol{\rho}'|^2}{2(z-z')}\right]\hat{\beta}_4^\dagger(\boldsymbol{\rho}',z') ,$$
$$\hat{\Omega}_{s2}^{(-)}(\boldsymbol{\rho},z)\sim\int dz'\int_{A'}d\boldsymbol{\rho}'\frac{1}{z-z'}k_4\exp\left[i\frac{\alpha_4^*(z-z')}{2k_4}+i\frac{k_4|\boldsymbol{\rho}-\boldsymbol{\rho}'|^2}{2(z-z')}\right]\hat{\beta}_4^\dagger(\boldsymbol{\rho}',z') . \tag{3.17}$$

We can repeat the same procedure as employed in Sec. II to calculate the far field using the Huygens principle. It is obvious that only appropriate substitutions are needed because of the exactly similar functional forms. We assume, as in Eq. (2.14),

$$\hat{\beta}_4{}^\dagger(\boldsymbol{\rho},z)=e^{-\rho^2}\bar{\hat{\beta}}_4^\dagger(\boldsymbol{\rho},z) . \tag{3.18}$$

A. Coherent source

We will take the following for $\hat{\beta}_4^\dagger$ as in Eq. (2.17),

$$\bar{\hat{\beta}}_4{}^\dagger(\boldsymbol{\rho},z)=\text{const} . \tag{3.19}$$

Then the far field can also be written as a sum of two parts

$$\hat{\Omega}_{s1}^{(-)}(\rho,Z)\sim k_s e^{-\rho^2/(\mathcal{F}_s Z)^2} e^{-i\eta/2}\frac{\sin\eta/2}{\eta} ,$$
$$\hat{\Omega}_{s2}^{(-)}(\rho,Z)\sim k_4 e^{-\rho^2/(\mathcal{F}_s Z)^2} e^{-i(\eta_4/2)}\frac{\sin\eta_4/2}{\eta_4} , \tag{3.20}$$

with

$$\eta_4=\bar{\alpha}_4^*-\frac{\mathcal{F}_s\rho^2}{(\mathcal{F}_s Z)^2} ,$$
$$\bar{\alpha}_4^*=\frac{\alpha_4^* L}{2k_s} . \tag{3.21}$$

Under the approximation $n_4\approx 1$, the second term will peak on axis, and gradually decrease in the transverse direction. However, the first term will give a conical structure exactly as in Eq. (2.19) but due to the presence of the second term, the contrast of the cone will now be reduced. Nevertheless, with the same coherent source, the angle we obtain from the pure 4WM is the same as from the pure Cherenkov radiation condition. In fact, as explicitly given in Eqs. (1.3) and (1.4), the quantum noises $\hat{\beta}_s$ and $\hat{\beta}_4^\dagger$ are correlated and both have the long coherence length. Thus the Cherenkov-type source and the 4WM source are intimately connected in a two-level atomic medium. The observations always contain *both* effects.

B. White-noise source

Now we can also study the white-noise case as in Sec. II Eq. (2.22), with

$$\langle\hat{\beta}_4^\dagger(\rho,z)\hat{\beta}_4(\rho',z')\rangle\sim\delta(z-z')\delta(\rho-\rho') . \tag{3.22}$$

We obtain

$$I_s(\rho,Z)=I_{s11}+I_{s22}+I_{s12}+I_{s21} , \tag{3.23}$$

with

$$I_{s11}\sim\langle\hat{\Omega}_{s1}^{(-)}(\rho,Z)\hat{\Omega}_{s1}^{(+)}(\rho,Z)\rangle ,$$
$$I_{s22}\sim\langle\hat{\Omega}_{s2}^{(-)}(\rho,Z)\hat{\Omega}_{s2}^{(+)}(\rho,Z)\rangle ,$$
$$I_{s12}\sim\langle\hat{\Omega}_{s1}^{(-)}(\rho,Z)\hat{\Omega}_{s2}^{(+)}(\rho,Z)\rangle , \tag{3.24}$$
$$I_{s21}=I_{s12}^\dagger\sim\langle\hat{\Omega}_{s2}^{(-)}(\rho,Z)\hat{\Omega}_{s1}^{(+)}(\rho,Z)\rangle .$$

I_{s11} and I_{s22} will give terms similar to Eq. (2.23), which are essentially flat in the transverse direction. The interference term is

$$I_{s12}(\rho,Z)\sim\int_A\int_A\exp\left[-i\frac{|\rho-\rho_1|^2}{\mathcal{F}_s Z}+i\frac{|\rho-\rho_2|^2}{\mathcal{F}_s Z}\right]d\rho_1 d\rho_2\int_0^1\frac{1}{z_1'^2}e^{-i(\bar{\alpha}_s+\bar{\alpha}_4^*)z_1'}dz_1'\int_{A'}$$
$$\times\exp\left[-i\frac{|\rho_1-\rho_1'|^2}{\mathcal{F}_s z_1'}-i\frac{|\rho_2-\rho_1'|^2}{\mathcal{F}_s z_1'}\right]e^{-2\rho_1'^2}d\rho_1' . \tag{3.25}$$

The integration over ρ_1 can be performed first as in Eq. (B2), while the integration over ρ_2 will be the same except for the substitution of $-Z$ for Z. Then we obtain

$$I_{s12}(\rho,Z)\sim-\int_0^1\int_{A'}\frac{1}{z_1'^2}dz_1' e^{-i(\bar{\alpha}_s z_1'+\bar{\alpha}_4^*)z_1'}\pi^2(\mathcal{F}_s z')^2 e^{2i[\rho^2\mathcal{F}_s z_1'/(\mathcal{F}_s Z)^2]}e^{-2\rho_1'^2}d\rho_1'$$
$$\sim-\int_0^1 e^{-i\eta_{s4}z_1'}dz_1'$$
$$=-2e^{-i(\eta_{s4}/2)}\frac{\sin(\eta_{s4}/2)}{\eta_{s4}} , \tag{3.26}$$

where

$$\eta_{s4}=\bar{\alpha}_a+\bar{\alpha}_4^*-\frac{2p^2\mathcal{F}_s}{(\mathcal{F}_s Z)^2} , \tag{3.27}$$

and similarly for I_{s21}.

The far-field intensity is then given by

$$I_s(\rho,Z)\sim\pi^3\mathcal{F}_s^2\left[1-\frac{\sin\eta_{s4}}{\eta_{s4}}\right] . \tag{3.28}$$

Under the approximation $n_4\approx 1$, we will see that the interference terms will give a minimum corresponding to $I_s(\rho,Z)=0$ along transverse direction at

$$\theta_c=\sqrt{\delta\eta_s} . \tag{3.29}$$

The first maximum will be roughly given by

$$\eta_{s4}=-\tfrac{3}{2}\pi , \tag{3.30}$$

with the corresponding angle at

$$\theta_c\approx\frac{\rho\rho_0}{ZL}=(\tfrac{1}{2})^{1/2}[(\bar{\alpha}_s+\tfrac{3}{2}\pi)\mathcal{F}_s]^{1/2}\frac{\rho_0}{L}$$
$$=\left[\delta n_s+\frac{3\pi}{2k_p L}\right]^{1/2} . \tag{3.31}$$

As seen from Fig. 4, the distribution does not look like a cone. However, the overall radial intensity variation, due to the diffraction envelope of the exit window, could make the resulting intensity distribution look something

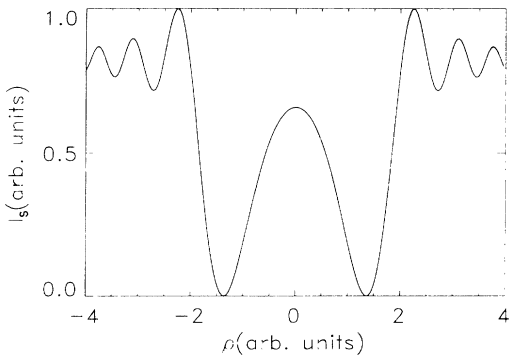

FIG. 4. Cross section of the far-field distribution resulting from the white-noise 4WM coupling. (The observed distribution is obtained when this result is multiplied by the diffraction envelope due to the exit aperture.)

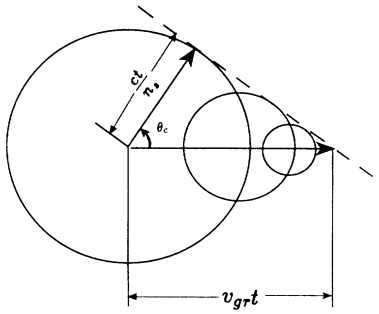

FIG. 5. Pure Cherenkov radiation scheme. The dashed line is the coherent-wave phase front.

like a "cone," with the cone angle given by Eq. (3.32). In most cases this "cone angle" is smaller than Eq. (2.21) which has an additional $\sqrt{2}$ factor. Since Valley *et al.* [9] used white noise in their calculations, we think this could be one of the reasons that the computed cones they obtained are about 20% smaller than the experimental ones. As we showed earlier, the δ-correlated noise in the $\hat{E}_s$ field equation will not give a cone. However, as seen from the above calculation, the δ-correlated noise in the $\hat{E}_4$ field equation enters the equation for $\hat{E}_s$ through the 4WM term, which effectively filters the white noise. This becomes in some sense a colored-noise source for the $\hat{E}_s$ field, and the spatial phase matching then leads to a modulation in the spatial intensity which under some circumstances has the appearance of a cone. We should also stress that Valley *et al.* [9] also explicitly included detailed transverse propagation effects which are known to give rise to cones in their own right.

IV. COMPARISON WITH OTHER MODELS

Since its experimental observation more than a decade ago, many theoretical and experimental works have dealt with the phenomenon of cone emission [1–7,9,11–20]. Some are highly numerical [9,12], with which we hope to compare in a future publication. However, many of the theoretical models are so simple that compact analytical formulas have been given. We compare them with our results in this section, and try to clarify some misunderstandings. We will write $n_j = n(\omega_j) = 1 + \delta n_j = 1 + \delta n(\omega_j)$.

The cone angle we obtain is

$$\theta_c = \sqrt{2(n_s - 1)} = \sqrt{2\delta n_s} \ . \tag{4.1}$$

Golub *et al.* [4] obtained a cone angle

$$\theta_c = \frac{v_{\rm ph}(\omega_s)}{v_{\rm gr}(\omega_p)} \tag{4.2}$$

according to the Cherenkov radiation condition (see Fig. 5), where $v_{\rm ph}(\omega_s)$ and $v_{\rm gr}(\omega_p)$ are the phase velocity of the possible generated field and the group velocity of the pump field, respectively. With $\delta n_p \approx 0$, the above can be reduced to

$$\theta_c = \frac{n_p}{n_s}\left[1 + \frac{\omega_p}{n_p}\frac{dn(\omega)}{d\omega}\bigg|_{\omega=\omega_p}\right] \approx \sqrt{2(\delta n_s - \delta n_p)} \approx \sqrt{2\delta n_s} \ . \tag{4.3}$$

This is consistent with our physical picture since our long-coherence-length source is equivalent to the Cherenkov source of Ref. [4]. Essentially the same formula was obtained by Plekhanov *et al.* [13]. They also studied the propagation of the field, which they attributed to a Cherenkov-type radiation, by requiring spatial phase matching with respect to the longitudinal coordinates they obtained,

$$\theta_c = \sqrt{2(n_s + n_4 - 2n_p)} \approx \sqrt{2\delta n_s} \ . \tag{4.4}$$

Again under the same approximations $n_p = n_4 = 1$, this reduces to Eq. (4.1).

LeBerre-Rousseau, Ressayre, and Tallet [14] obtained the same formula as Eq. (4.1) by a propagation study based on the transient atomic response. Their perturbative treatment for the field, when examined closely, can be seen to be equivalent to a long-coherence-length Cherenkov-type source.

Skinner and Kleiber [15] proposed a simple parametric 4WM model. Two additional parametric components were proposed to 4WM with the pump E_p and redshifted $\hat{E}_s$ fields. In such a process, if the fields involved are plane waves, energy and linear momentum conservation leads to

$$\begin{aligned} \omega_s &= \omega_p \pm \omega_1 \pm \omega_2 \ , \\ \mathbf{k}_s &= \mathbf{k}_p \pm \mathbf{k}_1 \pm \mathbf{k}_2 \ , \end{aligned} \tag{4.5}$$

where $k(\omega) = n(\omega)\omega/c$, with $n(\omega)$ being the refractive index at ω. They assumed that the redshifted component is the only one that will travel off axis (consequently linear momentum is not conserved in the transverse direction). With $n(\omega_1) = 1$ and $n(\omega_2) = 1$, they obtained

$$\begin{aligned} \omega_s &= \omega_p \pm \omega_1 \pm \omega_2 \ , \\ n(\omega_s)\omega_s \cos\theta_c &= n(\omega_p)\omega_p \pm \omega_1 \pm \omega_2 \ . \end{aligned} \tag{4.6}$$

With their assumption of $\delta n_s = -\delta n_p$ and $\omega_s \approx \omega_p$, the above gives a cone angle

$$\theta_c = 2\sqrt{\delta n_s} \ . \tag{4.7}$$

This seems to be $\sqrt{2}$ too big; however, if they had taken the same approximation $n_p \approx 1$, they would have obtained the same result as Eq. (4.1).

Harter *et al.* [5] based their theory on the parametric amplification of the Rabi sidebands. They observed that the fields E_p and $\hat{E}_4$ fields are essentially trapped in the self-focused filaments. Simple Snell's law refraction of the redshifted field $\hat{E}_s$ at the boundary of the trapped filaments gives

$$\theta_c = (\theta_0^2 + 2\delta n_s)^{1/2} \ , \tag{4.8}$$

with θ_0 the internal angle within the trapped filaments due to self-focusing or diffraction of the $\hat{E}_s$ field itself. It was assumed that inside the filaments, the index of refraction is 1 because of saturation. Again if further self-focusing is neglected (corresponding to $\hat{E}_s$ traveling almost along the axis in the filament) we may put $\theta_0 = 0$. Then Eq. (4.8) reduces Eq. (4.1) (see Fig. 6).

However, a pure plane-wave 4WM of the Rabi sidebands (see Fig. 7) would lead to

$$\begin{aligned} &2\omega_p = \omega_s + \omega_4 \ , \\ &n(\omega_s)\sin\theta_c = n(\omega_4)\sin\theta_4 \ , \\ &2n(\omega_p)\omega_p = n(\omega_s)\omega_s \cos\theta_s + n(\omega_4)\omega_4 \cos\theta_4 \ , \end{aligned} \tag{4.9}$$

which can be solved to give

$$\begin{aligned} \theta_4 &= \frac{n_s \omega_s}{n_4 \omega_4}\theta_c \ , \\ \theta_c &= \left[\frac{2(\delta n_s \omega_s + \delta n_4 \omega_4 - 2\delta n_p \omega_p)}{n_s \omega_s + \dfrac{n_s^2 \omega_s^2}{n_4 \omega_4}} \right]^{1/2} \\ &\approx \sqrt{\delta n_s + \delta n_4 - 2\delta n_p} \ . \end{aligned} \tag{4.10}$$

Here we have assumed that the pump field is propagating along the axis, and the self-focusing effect has been neglected. With $\delta n_4 = 0$ and $\delta n_p = 0$, Eq. (4.9) gives

$$\theta_c = \sqrt{\delta n_s} \ , \tag{4.11}$$

which is a factor of $\sqrt{2}$ smaller than Eq. (4.1). Similar formulas from 4WM were obtained for the two-photon pumped conical emission [16].

We can see that the pure plane-wave 4WM is not in agreement with the other models. Because unjustified approximations have been made, there is no reason to get the right answer. Based on the plane-wave assumption, 4WM allows both generated fields to travel off-axis, which is against experimental evidence. It also neglects the filamentation due to self-focusing, which proves to be crucial according to other model studies. Thus, although there are many different interpretations of the cone, it appears that most give the same cone angle under the approximation $n_p \approx 1$ and $n_4 \approx 1$.

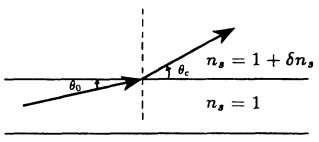

FIG. 6. Enhanced 4WM in the filament and refraction at the boundary of the filament (from Ref. [5]).

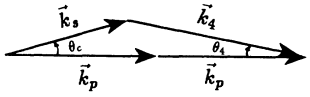

FIG. 7. Simple plane-wave 4WM scheme.

V. CONCLUSIONS

We have verified that a Cherenkov-type mechanism is also responsible for cone emission. In particular, by various model studies we are able to unify many of the previous simple models, and elucidate the important role of the long-coherence-length quantum-noise source. The long controversy between the 4WM and Cherenkov radiation models is resolved. For a two-level atomic medium, the Cherenkov-type and 4WM sources are in fact correlated, and are intimately mixed in the final observables. Thus in order to test the theory, different systems should be employed. We are currently examining both theoretically and experimentally a three-level Λ-type system in which the Cherenkov-type source but not the 4WM source occurs.

Many experimental studies have employed pulsed excitation. One important parameter that defines the steady-state limit is $\gamma\tau_p$, with τ_p being the duration of the pulse, and γ^{-1} the radiative decay time. If $\gamma\tau_p \gg 1$, we are basically in the steady state. If $\gamma\tau_p \sim 1$, then the initial condition terms (neglected in the present paper) will also contribute, and complications due to amplified spontaneous emission (ASE) and superfluorescence (SF) will arise. These emissions at the pump frequency could be resolved spectroscopically, and the physics for Cherenkov-type emission will still be applicable for the generated fields at a new frequency. Even if $\gamma\tau_p \ll 1$ we can still obtain solutions if we include the initial conditions, since the detuning Δ (or Rabi frequency) is large, as long as $\Delta\tau_p \gg 1$, the polarization will depend adiabatically on the inversion, and we could again expect new frequency fields to occur experimentally. In fact we should expect much the same physics although with a time-dependent coefficient due to the instantaneous inversion. On the other hand, if $\Delta\tau_p < 1$, the physics will probably be dominated by ASE or SF regimes, and then coherent counterpropagating waves will also be possible.

ACKNOWLEDGMENTS

The authors would like to thank R. Shuker for stimulating discussions, and G. S. Agarwal, K. Rzazewski, and

D. J. Gauthier for interesting conversations. One of us (J. M.) received support from the JILA Visiting Fellowship Program. One of us (L.Y.) would like to acknowledge J. W. Cooper, P. L. Knight, and J. Dailbard for helpful communications. This work is supported in part by NSF Grant No. PHY90-12244 through the University of Colorado.

APPENDIX A

From Eq. (2.1) we have

$$\left[\nabla_T^2-2ik_0\frac{\partial}{\partial z}\right]\hat{\Omega}(\boldsymbol{\rho},z)=-\alpha\hat{\Omega}(\boldsymbol{\rho},z)+\hat{\beta}(\boldsymbol{\rho},z)\ , \tag{A1}$$

$$\begin{aligned}&\mathbf{k}=k_0\hat{z}+\mathbf{K}\ ,\\&\mathbf{K}=\mathbf{K}_\perp+\mathbf{K}_\parallel\ ,\end{aligned} \tag{A2}$$

where the part of the wave number corresponding to the slowly varying propagation is $\mathbf{K}$. We Fourier transform the above equation with respect to the transverse coordinate $\boldsymbol{\rho}$ according to

$$\begin{aligned}\hat{\Omega}(\mathbf{K}_\perp,z)&=\frac{1}{2\pi}\int_{A'}e^{i\mathbf{K}_\perp\cdot\boldsymbol{\rho}}\hat{\Omega}(\boldsymbol{\rho},z)d\boldsymbol{\rho}\ ,\\\hat{\beta}(\mathbf{K}_\perp,z)&=\frac{1}{2\pi}\int_{A'}e^{i\mathbf{K}_\perp\cdot\boldsymbol{\rho}}\hat{\beta}(\boldsymbol{\rho},z)d\boldsymbol{\rho}\ .\end{aligned} \tag{A3}$$

Here A' is the two-dimensional transverse plane across the cell. $\overline{A}'$ is the corresponding plane in momentum space. We then get the following:

$$-2ik_0\frac{\partial}{\partial z}\hat{\Omega}(\mathbf{K}_\perp,z)=(\mathbf{K}_\perp^2-\alpha)\hat{\Omega}(\mathbf{K}_\perp,z)+\hat{\beta}(\mathbf{K}_\perp,z)\ , \tag{A4}$$

the solution of which is

$$\begin{aligned}\hat{\Omega}(\mathbf{K}_\perp,z)=\hat{\Omega}(\mathbf{K}_\perp,0)e^{i[(K_\perp^2-\alpha)/2k_0]z}\\+\int_0^z e^{i[(K_\perp^2-\alpha)/2k_0](z-z')}\hat{\beta}(\mathbf{K}_\perp,z')dz'\ .\end{aligned} \tag{A5}$$

Applying the inverse Fourier transformation, we obtain

$$\begin{aligned}\hat{\Omega}(\boldsymbol{\rho},z)=&\frac{1}{(2\pi)^2}\int_{\overline{A}'}e^{-i\mathbf{K}_\perp\cdot(\boldsymbol{\rho}-\boldsymbol{\rho}')}d\mathbf{K}_\perp e^{i[(K_\perp^2-\alpha)/2k_0]z}\int_{A'}\hat{\Omega}(\boldsymbol{\rho}',0)d\boldsymbol{\rho}'\\&+\frac{1}{(2\pi)^2}\int_{\overline{A}'}e^{-i\mathbf{K}_\perp\cdot(\boldsymbol{\rho}-\boldsymbol{\rho}')}d\mathbf{K}_\perp\int_0^z e^{i[(K_\perp^2-\alpha)/2k_0](z-z')}dz'\int^{A'}\hat{\beta}(\boldsymbol{\rho}',z)d\boldsymbol{\rho}'\ ,\end{aligned} \tag{A6}$$

with

$$\begin{aligned}\int_{\overline{A}'}e^{i[(K_\perp^2-\alpha)/2k_0](z-z')}e^{i\mathbf{K}_\perp\cdot(\boldsymbol{\rho}-\boldsymbol{\rho}')}d\mathbf{K}_\perp&=e^{-(i\alpha/2k_0)(z-z')}\int_0^\infty e^{i(K_\perp^2/2k_0)(z-z')}\int_0^{2\pi}e^{-iK_\perp|\boldsymbol{\rho}-\boldsymbol{\rho}'|\cos\theta}K_\perp dK_\perp d\theta\\&=e^{-(i\alpha/2k_0)(z-z')}\int_0^\infty e^{i(K_\perp^2/2k_0)(z-z')}(2\pi)J_0(K_\perp|\boldsymbol{\rho}-\boldsymbol{\rho}'|)K_\perp dK_\perp\\&=\frac{2ik_0\pi}{z-z'}e^{-(i\alpha/2k_0)(z-z')}e^{-i[k_0|\boldsymbol{\rho}-\boldsymbol{\rho}'|^2/2(z-z')]}\ ,\end{aligned} \tag{A7}$$

where θ is the angle between $\mathbf{K}_\perp$ and $\boldsymbol{\rho}-\boldsymbol{\rho}'$. Thus we obtain the general solution of Eq. (A1)

$$\begin{aligned}\hat{\Omega}(\boldsymbol{\rho},z)=&\frac{ik_0}{2\pi z}e^{-i\alpha z/2k_0}\int_{A'}e^{-i(k_0|\boldsymbol{\rho}-\boldsymbol{\rho}'|^2/2z)}\hat{\Omega}(\boldsymbol{\rho}',0)d\boldsymbol{\rho}'\\&+\frac{ik_0}{2\pi}\int_0^z\int_{A'}\frac{1}{z-z'}e^{-(i\alpha/2k_0)(z-z')}e^{-i[k_0|\boldsymbol{\rho}-\boldsymbol{\rho}'|^2/2(z-z')]}\hat{\beta}(\boldsymbol{\rho}',z')dz'd\boldsymbol{\rho}'\ .\end{aligned} \tag{A8}$$

APPENDIX B

From Eq. (2.18) we have

$$\overline{\hat{\Omega}}_s^{(-)}(\boldsymbol{\rho},Z)\sim\int_A e^{-i(|\boldsymbol{\rho}-\boldsymbol{\rho}_1|^2/\mathcal{F}_sZ)}d\boldsymbol{\rho}_1\int_0^1\int_{A'}\frac{1}{z'}e^{-i\bar{\alpha}_sz'}e^{-i(|\boldsymbol{\rho}_1-\boldsymbol{\rho}_1'|^2/\mathcal{F}_sz')}e^{-\rho'^2}dz'd\boldsymbol{\rho}_1'\ . \tag{B1}$$

The integration over $\boldsymbol{\rho}'$ can be done first as

$$\begin{aligned}\int_{A'}e^{-i(|\boldsymbol{\rho}_1-\boldsymbol{\rho}_1'|^2/\mathcal{F}_sz')}e^{-\rho'^2}d\boldsymbol{\rho}_1'&=e^{-i(\rho_1^2/\mathcal{F}_sz')}\int_{A'}\int_0^{2\pi}e^{-(1+i/\mathcal{F}_sz')\rho'^2+\frac{2i\rho_1\rho_1'\cos\theta_1}{\mathcal{F}_sz'}}\rho_1'd\rho_1'd\theta_1\\&=e^{-i(\rho_1^2/\mathcal{F}_sz')}(2\pi)\int_{A'}e^{-(1+i/\mathcal{F}_sz')\rho'^2}J_0\left[\frac{2\rho_2\rho_1'}{\mathcal{F}_sz'}\right]\rho_1'd\rho_1'\\&=\frac{\pi}{1+\frac{i}{\mathcal{F}_sz'}}e^{-i\rho_1^2/(i+\mathcal{F}_sz')}\ ,\end{aligned} \tag{B2}$$

where θ_1 is the angle between $\boldsymbol{\rho}_1$ and $\boldsymbol{\rho}_1'$. Substituting into Eq. (B1), we have

$$\bar{\hat{\Omega}}_s^{(-)}(\boldsymbol{\rho},Z)\sim\int_A e^{-i(|\boldsymbol{\rho}-\boldsymbol{\rho}_1|^2/\mathcal{F}_sZ)}d\boldsymbol{\rho}_1\int_0^1\frac{\pi}{z'+\frac{i}{\mathcal{F}_s}}e^{-i\bar{\alpha}_sz'}\exp[-i\rho_1^2/(i+\mathcal{F}_sz')]dz' . \tag{B3}$$

Changing the order of integration, we see that the $\bar{\rho}_1$ integration can be explicitly performed as in Eq. (B2)

$$\int_A e^{-i(|\boldsymbol{\rho}-\boldsymbol{\rho}_1|^2/\mathcal{F}_sZ)}e^{-i\rho_1^2/(i+\mathcal{F}_sz')}d\boldsymbol{\rho}_1=\frac{\pi}{\left[\frac{1}{1-i\mathcal{F}_sz'}+\frac{i}{\mathcal{F}_sZ}\right]}e^{-i(\rho^2/\mathcal{F}_sZ)}\exp\left[-\frac{\rho^2}{(\mathcal{F}_sZ)^2\left[\frac{1}{1-i\mathcal{F}_sz'}+\frac{i}{\mathcal{F}_sZ}\right]}\right] . \tag{B4}$$

We have then

$$\bar{\hat{\Omega}}_s^{(-)}(\boldsymbol{\rho},Z)\sim e^{-i(\rho^2/\mathcal{F}_sZ)}\int_0^1\frac{\pi^2}{\frac{i}{\mathcal{F}_sZ}\left[z'+\frac{i}{\mathcal{F}_s}\right]+\frac{i}{\mathcal{F}_s}}\exp\left[-i\bar{\alpha}_sz'-\frac{\rho^2}{\frac{(\mathcal{F}_sZ)^2}{1-i\mathcal{F}_sz'}+i\mathcal{F}_sZ}\right]dz' . \tag{B5}$$

This integration cannot be done explicitly. However, the polynomial term

$$\frac{\pi^2}{\frac{i}{\mathcal{F}_sZ}\left[z'+\frac{i}{\mathcal{F}_s}\right]+\frac{i}{\mathcal{F}_s}} \tag{B6}$$

is slowly varying, as $Z\gg z'\in[0,1]$. Then we obtain

$$\bar{\hat{\Omega}}_s^{(-)}(\boldsymbol{\rho},Z)\sim e^{-i(\rho^2/\mathcal{F}_sZ)}\frac{\pi^2}{\frac{i}{\mathcal{F}_sZ}\left[\epsilon+\frac{i}{\mathcal{F}_s}\right]+\frac{i}{\mathcal{F}_s}}\int_0^1\exp\left[-i\bar{\alpha}_sz'-\frac{\rho^2}{\frac{(\mathcal{F}_sZ)^2}{1-i\mathcal{F}_sz'}+i\mathcal{F}_sz}\right]dz' , \tag{B7}$$

where $\epsilon\in[0,1]$. For the terms in the exponent,

$$\left|\frac{(\mathcal{F}_sZ)^2}{1-i\mathcal{F}_sz'}\right|\gg\mathcal{F}_sZ , \tag{B8}$$

and we can then approximate

$$\exp\left[-\frac{\rho^2}{\frac{(\mathcal{F}_sZ)^2}{1-i\mathcal{F}_sz'}+i\mathcal{F}_sz}\right]\approx\exp\left[-\frac{\rho^2}{\frac{(\mathcal{F}_sZ)^2}{1-i\mathcal{F}_sz'}}\right]=\exp\left[-\frac{(1-i\mathcal{F}_sz')\rho^2}{(\mathcal{F}_sZ)^2}\right] . \tag{B9}$$

Finally we obtain

$$\bar{\hat{\Omega}}_s^{(-)}(\boldsymbol{\rho},Z)\sim\int_0^1 e^{-i\bar{\alpha}_sz'-(1-i\mathcal{F}_sz')\rho^2/(\mathcal{F}_sZ)^2}dz'=e^{-\rho^2/(\mathcal{F}_sZ)^2}e^{-i(\eta/2)}\frac{2\sin(\eta/2)}{\eta} , \tag{B10}$$

with

$$\eta=\bar{\alpha}_s-\frac{\mathcal{F}_s\rho^2}{(\mathcal{F}_sZ)^2} . \tag{B11}$$

APPENDIX C

From Eq. (2.22) we have

$$\langle\bar{\hat{\beta}}_s(\boldsymbol{\rho},z)\bar{\hat{\beta}}_s^{\dagger}(\boldsymbol{\rho}',z')\rangle\sim\delta(\boldsymbol{\rho}-\boldsymbol{\rho}')\delta(z-z') \tag{C1}$$

so that

$$I_s(\boldsymbol{\rho},Z)\sim\langle\bar{\hat{\Omega}}_s^{(-)}(\boldsymbol{\rho},Z)\bar{\hat{\Omega}}_s^{(+)}(\boldsymbol{\rho},Z)\rangle$$
$$\sim\int_A\int_A\exp\left[-i\frac{|\boldsymbol{\rho}-\boldsymbol{\rho}_1|^2}{\mathcal{F}_sZ}+i\frac{|\boldsymbol{\rho}-\boldsymbol{\rho}_2|^2}{\mathcal{F}_sZ}\right]d\boldsymbol{\rho}_1d\boldsymbol{\rho}_2\int_0^1\frac{1}{z_1'^2}dz_1'\int_{A'}\exp\left[-i\frac{|\boldsymbol{\rho}_1-\boldsymbol{\rho}'|^2}{\mathcal{F}_sz_1'}+i\frac{|\boldsymbol{\rho}_2-\boldsymbol{\rho}_1'|^2}{\mathcal{F}_sz_1'}\right]e^{-2\rho_1'^2}d\boldsymbol{\rho}_1' . \tag{C2}$$

The integration over $\boldsymbol{\rho}_1$ and $\boldsymbol{\rho}_2$ can be done as in Eq. (B2). Thus

$$\int_A e^{-i(|\boldsymbol{\rho}-\boldsymbol{\rho}_1|^2/\mathcal{F}_sZ)}e^{-i(|\boldsymbol{\rho}_1-\boldsymbol{\rho}_1'|^2/\mathcal{F}_sz_1')}d\boldsymbol{\rho}_1=\frac{\pi}{i\left[\frac{1}{\mathcal{F}_sZ}+\frac{1}{\mathcal{F}_sz_1'}\right]}\exp\left[-i\frac{\rho^2}{\mathcal{F}_sZ}-i\frac{\rho_1'^2}{\mathcal{F}_sz_1'}\right]\exp\left[i\frac{\left|\frac{\boldsymbol{\rho}}{\mathcal{F}_sZ}+\frac{\boldsymbol{\rho}_1'}{\mathcal{F}_sz_1'}\right|^2}{\left[\frac{1}{\mathcal{F}_sZ}+\frac{1}{\mathcal{F}_sz_1'}\right]}\right], \tag{C3}$$

$$\int_A e^{i(|\boldsymbol{\rho}-\boldsymbol{\rho}_2|^2/\mathcal{F}_sZ)}e^{i(|\boldsymbol{\rho}_2-\boldsymbol{\rho}_1'|^2/\mathcal{F}_sz_1')}d\boldsymbol{\rho}_2=\frac{i\pi}{\left[\frac{1}{\mathcal{F}_sZ}+\frac{1}{\mathcal{F}_sz_1'}\right]}\exp\left[i\frac{\rho^2}{\mathcal{F}_sZ}+i\frac{\rho_1'^2}{\mathcal{F}_sz_1'}\right]\exp\left[-i\frac{\left|\frac{\boldsymbol{\rho}}{\mathcal{F}_sZ}+\frac{\boldsymbol{\rho}_1'}{\mathcal{F}_sz_1'}\right|^2}{\left[\frac{1}{\mathcal{F}_sZ}+\frac{1}{\mathcal{F}_sz_1'}\right]}\right].$$

Substituting into Eq. (C2), we obtain

$$I_s(\boldsymbol{\rho},Z)\sim\int_0^1\frac{1}{z_1'^2}dz_1'\int_{A'}\frac{\pi^2}{\left[\frac{1}{\mathcal{F}_sZ}+\frac{1}{\mathcal{F}_sz'}\right]^2}e^{-2\rho_1'^2}d\boldsymbol{\rho}_1'$$
$$=\int_0^1\frac{\pi^3}{2\left[\frac{z'}{\mathcal{F}_sZ}+\frac{1}{\mathcal{F}_s}\right]^2}dz_1'$$
$$=\frac{\pi^3\mathcal{F}_s^2Z}{2(1+z)} . \tag{C4}$$

APPENDIX D

From Eq. (2.25) we have

$$\langle\bar{\hat{\beta}}_s(\boldsymbol{\rho},z)\bar{\hat{\beta}}_s^{\dagger}(\boldsymbol{\rho}',z')\rangle\sim e^{-(1/\lambda_\perp)|\boldsymbol{\rho}-\boldsymbol{\rho}'|}e^{-(1/\lambda_\parallel)|z-z'|} . \tag{D1}$$

We find

$$I_s(\boldsymbol{\rho},Z)\sim\int_A\int_A\exp\left[-i\frac{|\boldsymbol{\rho}-\boldsymbol{\rho}_1|^2}{\mathcal{F}_sZ}+i\frac{|\boldsymbol{\rho}-\boldsymbol{\rho}_2|^2}{\mathcal{F}_sZ}\right]d\boldsymbol{\rho}_1d\boldsymbol{\rho}_2$$
$$\times\int_0^1\int_0^1\frac{1}{z_1'z_2'}e^{-i\bar{\alpha}_sz_1'+i\bar{\alpha}_sz_2'}dz_1'dz_2'$$
$$\times\int_{A'}\int_{A'}\exp\left[-i\frac{|\boldsymbol{\rho}_1-\boldsymbol{\rho}_1'|^2}{\mathcal{F}_sz_1'}+i\frac{|\boldsymbol{\rho}_2-\boldsymbol{\rho}_2'|^2}{\mathcal{F}_sz_2'}\right]d\boldsymbol{\rho}_2'd\boldsymbol{\rho}_2'e^{-\rho_1'^2-\rho_2'^2}e^{-(1/\lambda_\perp)|\boldsymbol{\rho}_1'-\boldsymbol{\rho}_2'|}e^{-(1/\lambda_\parallel)|z_1'-z_2'|} . \tag{D2}$$

The integration over $\boldsymbol{\rho}_1$ and $\boldsymbol{\rho}_2$ is given in Eq. (C3). Substituting into Eq. (D2), we obtain

$$I_s(\boldsymbol{\rho},Z)\sim\int_0^1\int_0^1 e^{-i\bar{\alpha}_s z_1'+i\bar{\alpha}_s z_2'}dz_1'dz_2'$$
$$\times\int_{A'}\int_{A'}d\boldsymbol{\rho}_1'd\boldsymbol{\rho}_2' e^{-(1/\lambda_\perp)|\boldsymbol{\rho}_1'-\boldsymbol{\rho}_2'|}e^{-(1/\lambda_\parallel)|z_1'-z_2'|}\frac{1}{(1+z_1'/Z)(1+z_2'/Z)}$$
$$\times e^{-\rho_1'^2-\rho_2'^2}\exp\left[-i\frac{\rho_1'^2-2\boldsymbol{\rho}_1'\cdot\boldsymbol{\rho}-(z_1'/Z)\rho^2}{\mathcal{F}_s(Z+z_1')}\right]\exp\left[i\frac{\rho_2'^2-2\boldsymbol{\rho}_2'\cdot\boldsymbol{\rho}-(z_2'/Z)\rho^2}{\mathcal{F}_s(Z+z_2')}\right]. \tag{D3}$$

Since $z_i'\ll Z$, we can put $1+z_i'/Z\approx 1$, to obtain

$$I_s(\boldsymbol{\rho},Z)\sim\int_0^1\int_0^1 e^{-i\bar{\alpha}_s z_1'+i\bar{\alpha}_s z_2'}e^{i(\rho^2/\mathcal{F}_s Z^2)z_1'}e^{-i(\rho^2/\mathcal{F}_s Z^2)z_2'}e^{-(1/\lambda_\parallel)|z_1'-z_2'|}dz_1'dz_2'$$
$$\times\int_{A'}\int_{A'}e^{-\rho_1'^2-\rho_2'^2}\exp\left[-i\frac{\rho_1'^2-2\boldsymbol{\rho}_1'\cdot\boldsymbol{\rho}}{\mathcal{F}_s Z}\right]\exp\left[i\frac{\rho_2'^2-2\boldsymbol{\rho}_2'\cdot\boldsymbol{\rho}}{\mathcal{F}_s Z}\right]e^{-(1/\lambda_\perp)|\boldsymbol{\rho}_1'-\boldsymbol{\rho}_2'|}d\boldsymbol{\rho}_1'd\boldsymbol{\rho}_2'$$
$$=\mathcal{R}Z\ , \tag{D4}$$

where

$$\mathcal{R}=\int_{A'}\int_{A'}e^{-\rho_1'^2-\rho_2'^2}\exp\left[-i\frac{\rho_1'^2-2\boldsymbol{\rho}_1'\cdot\boldsymbol{\rho}}{\mathcal{F}_s Z}\right]\exp\left[i\frac{\rho_2'^2-2\boldsymbol{\rho}_2'\cdot\boldsymbol{\rho}}{\mathcal{F}_s Z}\right]e^{-(1/\lambda_\perp)|\boldsymbol{\rho}_1'-\boldsymbol{\rho}_2'|}d\boldsymbol{\rho}_1'd\boldsymbol{\rho}_2'\ ,$$
$$Z=\int_0^1\int_0^1 e^{-i(\bar{\alpha}_s-\rho^2/\mathcal{F}_s Z^2)(z_1'-z_2')}e^{-(1/\lambda_\parallel)|z_1'-z_2'|}dz_1'dz_2'\ . \tag{D5}$$

Changing the integration variable in $\mathcal{R}$ from $\boldsymbol{\rho}_2'$ to $\boldsymbol{\rho}'=\boldsymbol{\rho}_2'-\boldsymbol{\rho}_1'$, we get

$$\mathcal{R}=\int_{A'}\int_{A'}e^{-\rho_1'^2-|\boldsymbol{\rho}'+\boldsymbol{\rho}_1'|^2}\exp\left[-i\frac{\rho_1'^2-|\boldsymbol{\rho}'+\boldsymbol{\rho}_1'|^2}{\mathcal{F}_s Z}\right]e^{-2i(\boldsymbol{\rho}\cdot\boldsymbol{\rho}'/\mathcal{F}_s Z)}e^{-(1/\lambda_\perp)\rho'}d\boldsymbol{\rho}_1'd\boldsymbol{\rho}'\ . \tag{D6}$$

The integration over $\boldsymbol{\rho}_1'$ is the same as in Eq. (B4), and gives

$$\int_{A'}e^{-\rho_1'^2-|\boldsymbol{\rho}'+\boldsymbol{\rho}_1'|^2}\exp\left[-i\frac{\rho_1'^2-|\boldsymbol{\rho}'+\boldsymbol{\rho}_1'|^2}{\mathcal{F}_s Z}\right]d\boldsymbol{\rho}'_1=\frac{\pi}{2}\exp\left[-\left[1-\frac{i}{\mathcal{F}_s Z}\right]\rho'^2\right]\exp\left[-\left[i+\frac{1}{\mathcal{F}_s Z}\right]^2\rho'^2\right]. \tag{D7}$$

On substitution back into Eq. (D6), we obtain

$$\mathcal{R}\sim\int_{A'}\exp\left[-\left[1-\frac{i}{\mathcal{F}_s Z}\right]\rho'^2\right]\exp\left[-\left[i+\frac{1}{\mathcal{F}_s z}\right]^2\rho'^2\right]e^{-2i(\boldsymbol{\rho}\cdot\boldsymbol{\rho}'/\mathcal{F}_s Z)}e^{-(1/\lambda_\perp)\rho'}d\boldsymbol{\rho}'$$
$$=\int_0^\infty\int_0^{2\pi}\exp\left[-\left[1-\frac{i}{\mathcal{F}_s Z}\right]\rho'^2-\left[i+\frac{1}{\mathcal{F}_s Z}\right]^2\rho'^2\right]e^{-2i(\rho\rho'\cos\theta'/\mathcal{F}_s Z)}e^{-(1/\lambda_\perp)\rho'}\rho'd\rho'd\theta'$$
$$=2\pi\int_0^\infty\exp\left[-\left[1-\frac{i}{\mathcal{F}_s Z}\right]\rho'^2-\left[i+\frac{1}{\mathcal{F}_s Z}\right]^2\rho'^2\right]J_0\left[2\frac{\rho\rho'}{\mathcal{F}_s Z}\right]e^{-(1/\lambda_\perp)\rho'}\rho'd\rho'\ . \tag{D8}$$

---

*Also at Department of Physics, University of Colorado, Boulder, CO 80309-0390.

†Permanent address: Institute of Physics, Polish Academy of Sciences, Aleja Lotnikow 32, 02-668 Warszawa, Poland.

[1] D. Grischkowsky, Phys. Rev. Lett. **24**, 866 (1970).

[2] A. C. Tam, Phys. Rev. A **19**, 1971 (1979).

[3] L. You, J. Mostowski, J. Cooper, and R. Shuker, Phys. Rev. A **44**, 6998 (1991).

[4] I. Golub, R. Shuker, and G. Erez, Opt. Commun. **34**, 439 (1980); I. Golub, G. Erez, and R. Shuker, J. Phys. B **19**, L115 (1986).

[5] D. J. Harter, P. Narum, M. G. Raymer, and R. W. Boyd, Phys. Rev. Lett. **46**, 1192 (1981); D. J. Harter and R. W. Boyd, Phys. Rev. A **29**, 739 (1984).

[6] A. W. McCord, R. J. Ballagh, and J. Cooper, J. Opt. Soc. Am. B **5**, 1323 (1988).

[7] M. Comte, H. Graillot, and Ph. Kupecek, Opt. Commun. **79**, 235 (1990).

[8] L. You, J. Mostowski, and J. Cooper, preceding paper, Phys. Rev. A **46**, 2903 (1992).

[9] J. F. Valley, G. Khitrova, H. M. Gibbs, J. W. Grantham, and Xu Jiajin, Phys. Rev. Lett. **64**, 2362 (1990).

[10] M. Born and W. Wolf, *The Principle of Optics,* 4th ed. (Pergamon, New York, 1970).

[11] NBS *Handbook of Mathematical Functions With Formulas, Graphs, and Mathematical Tables,* edited by M.

Abramowitz and I. E. Stegun, Natl. Bur. Stand. Appl. Math. Ser. No. 55 (GPO, Washington, D. C. 1968).
[12] M. E. Crenshaw and C. D. Cantrell, Phys. Rev. A **39**, 126 (1989).
[13] A. I. Plekhanov, S. G. Rautian, V. P. Safonov, and B. M. Chernobrod, Zh. Eksp. Teor. Fiz. **88**, 426 (1985) [Sov. Phys. JETP **61**, 249 (1985)].
[14] M. LeBerre-Rousseau, E. Ressayre, and A. Tallet, Opt. Commun. **36**, 31 (1981).
[15] C. H. Skinner and P. D. Kleiber, Phys. Rev. A **21**, 151 (1980); C. H. Skinner, Opt. Commun. **41**, 255 (1982).
[16] J. Krasinski, D. J. Gauthier, M. S. Malcuit, and R. W. Boyd, Opt. Commun. **54**, 241 (1985).
[17] Y. Shevy and M. Rosenbluh, J. Opt. Soc. Am. B **5**, 116 (1988).
[18] Y. H. Meyer, Opt. Commun. **57**, 143 (1986); J. Phys. B **20**, L63 (1987).
[19] G. Brechnignac, Ph. Cahuzac, and A. Debarre, Opt. Commun. **35**, 87 (1980).
[20] J. Pender and L. Hesselink, J. Opt. Soc. Am. B **7**, 1361 (1990).